Influence of the anode materials on the electrochemical oxidation efficiency. Application to oxidative degradation of the pharmaceutical amoxicillin

Flamur Sopaj[a,b], Manuel A. Rodrigo[c], Nihal Oturan[a], Fetah I. Podvorica[b], Jean Pinson[d], Mehmet A. Oturan[a,*]

[a] *Université Paris-Est, Laboratoire Géomatériaux et Environnement (LGE), UPEM, 77454 Marne-la-Vallée Cedex 2, France*

[b] *Chemistry Department of Natural Sciences Faculty, University of Prishtina, rr. "Nëna Tereze" nr. 5, 10 000 Prishtina, Kosovo*

[c] *University of Castilla La Mancha, Department of Chemical Engineering, Faculty of Chemical Sciences, E-13071 Ciudad Real, Spain*

[d] *Univ Paris Diderot, Sorbonne Paris Cité, ITODYS, UMR 7086 CNRS, 15 rue J-A de Baïf, 75205 Paris, Cedex 13, France*

Paper submitted for consideration to *Chemical Engineering Journal*

* Corresponding Author:

E-mail: Mehmet.Oturan@univ-paris-est.fr

Phone: +33 149 32 90 65

Abstract

In this study, the electro-oxidation capacities of several electrode materials such as carbon-felt, carbon-fiber, carbon-graphite, platinum, lead dioxide, DSA (Dimensionally Stable Anode), (Ti/RuO_2-IrO_2), and BDD (Boron-Doped Diamond) were tested for the destruction of the antibiotic amoxicillin (AMX) in aqueous medium. BDD anode was more efficient than DSA to oxidize and mineralize totally AMX in water. Moreover, for BDD electrode we obtained very high electrolysis efficiency for the initial stage of the process even for high current densities which is an indirect indicator that mediated oxidation is involved in the whole degradation of AMX. By considering the oxidation reactions under mass transfer control, the apparent rate constants for oxidation of AMX by hydroxyl radicals were determined for all anode materials tested. The data obtained showed that in all cases the oxidation rate constants depended mainly on applied current densities for each material. Platinum showed a relatively good oxidation behavior compared to carbon-fiber and carbon-graphite. DSA was found to be the less efficient electrode for oxidation of AMX. BDD was evidenced as the best anode material at high current densities due to the formation of large amounts of hydroxyl radicals and of different other oxidants such as hydrogen peroxide, ozone and persulfates that contribute to enhancement of oxidation and mineralization of AMX via mediated oxidation.

Keywords: Electro-oxidation, Oxidation power, Amoxicillin, BDD, Carbon-felt, PbO_2, Mineralization

1. Introduction

Human beings, during their activities in everyday life, use many synthetic chemicals that may pollute water and cause many adverse effects to the environment. For this reason, wastewaters containing harmful chemicals have to be treated to remove the toxic constituents before their disposal in natural water streams. In recent years, several wastewater treatment methods have been developed to remove toxic and biorefractory organic pollutants from wastewater [1-4]. Among these methods, a great attention has been paid to the Advanced Oxidation Processes (AOPs) that are based on the in situ production and the reactivity of a very reactive species, the hydroxyl radical ($^{\bullet}OH$) which is a powerful oxidizing agent [5-10]. $^{\bullet}OH$ produced by AOPs is able to react non-selectively with any persistent organic pollutant and oxidize them to their almost complete mineralization (conversion of organic carbon to CO_2). Nevertheless, many of these methods require the use of chemicals like H_2O_2, O_3, $FeSO_4$, etc., which are associated to potential hazards of storage and handling, and sometimes with the occurrence of reduction products in treated wastes.

In this context, the AOPs based on electrochemical technology have attracted growing interest as alternative to traditional methods [11-16] as simple, economical, safe and environmentally compatible technologies for treatment of polluted water. Thus, the main reagent in Electrochemical Advanced Oxidation Processes (EAOPs) is electrical current and these technologies do not use harmful chemicals to produce strong oxidants. One of the most popular EAOPs is the electro-oxidation or anodic oxidation (AO) in which organic pollutants are oxidized by heterogeneous hydroxyl radicals M($^{\bullet}OH$) produced at anode (M) surface from water discharge (Eq. (1)) [17-21].

$$M + H_2O \rightarrow M(^{\bullet}OH) + H^+ + e^- \quad (1)$$

Formed M($^{\bullet}OH$) are then responsible of the oxidation of organics (R) until overall mineralization (transformation them to CO_2 and water) [22-27] as shown in the following general reaction:

$$M(^{\bullet}OH) + R \rightarrow M + \text{oxidation intermediates} \quad (2)$$

$$\text{Intermediates} + M(^{\bullet}OH) \rightarrow M + CO_2 + H_2O + \text{inorganic ions} \quad (3)$$

AO process generates, in addition to M(•OH), several oxidant species, that contribute to oxidation process in bulk. The extent of these oxidants involved in mediated oxidation depends on the nature of the supporting electrolyte. For example the use of Na_2SO_4, or NaCl as supporting electrolyte leads to the formation of oxidants persulfate ($S_2O_8^{2-}$) or hypochlorite (ClO^-) ions, respectively, contributing to the oxidation of initial pollutant or its oxidation intermediates therefore increasing mineralization efficiency of the process [17, 23, 24, 29-31]. The generation of these oxidants is particularly characteristic of high oxygen overvoltage anodes like BDD (Boron-Doped Diamond) and lead dioxide [17, 32, 33].

On the other hand, the oxidizing power of M(•OH) generated by an AO process depends on the nature of M. For example, BDD(•OH) is significantly more efficient in terms of oxidation/mineralization of organics than Pt(•OH), since •OH are physisorbed on the former but chemisorbed on the later [34-36]. It was also shown that the anodes having high O_2 overpotential give better results in AO [37-43]. Therefore, the electrode material (M) has an important impact in oxidative degradation efficiency of organic pollutants. Consequently, a systematic research on comparative performance of electrode materials available as anode is an interesting issue of EAOPs. Only a limited number of papers tried to compare the oxidation power of few number of anode materials. To the best of our knowledge, there was not any report measuring comparative performance of a large series of anode materials, but only works in which the comparison was carried out in terms of a one-to-one or small series of anodes. Therefore, in this study we undertook a comparative investigation on the oxidation power and mineralization efficiency of a series of available anodes (carbon-felt, carbon-fiber, carbon-graphite, platinum, lead dioxide, DSA (Dimensionally Stable Anode, Ti/RuO_2-IrO_2) and BDD versus a stainless steel cathode, under same experimental conditions. This series included the most studied materials in last three decades for electrochemical removal of organics contained in water and wastewater. The performance of the different anode materials was assessed by comparing the apparent rate constant values and TOC (Total Organic Carbon) removal efficiencies for the oxidative degradation of a widely used human and veterinary medicine, the amoxicillin (AMX) (Fig. 1), a semi-synthetic beta-lactam antibiotic, with good characteristics to be used as model emerging pollutant, because it is one of the antibiotics most frequently found in surface water at higher concentration than other pharmaceuticals [44, 45]. However, the concentrations of AMX used in this study were much higher than

the concentrations contained in surface and groundwater (in fact they can only be representative of industrial waste flows). In this work we were focused only on the performance of the electrochemical technology for degradation of this drug, aiming to compare the performance of different electrode materials, but not on the application to a real case. The key point was to propose a simple mathematical model to explain the electrochemical degradation of large number of molecules with different electrodes and efficiencies. The model fitted well to the experimental results demonstrating that assumptions taken into account were valid. The main novelty was the demonstration that electrochemical oxidation is mostly due to mediated oxidation processes and that direct processes have a very low impact in spite of having being used to explain the electrolysis of many organics in the past. Differences between electrode materials should be related to the nature and amount of oxidants produced at the anode surface and not to the direct electrochemical processes that may occur on their surface. Variation of the kinetic constants with the current density applied supports this novelty.

2. Experimental

2.1. Chemicals

Amoxicillin (AMX), $C_{16}H_{19}N_3O_5S$ ($\geq$ 97% purity) was provided by Fluka and used without any further purification. Methanol and acetic acid used in preparation of HPLC eluents, and Na_2SO_4 (> 99% purity) as supporting electrolyte were Sigma- Aldrich and Acros products. HPLC eluents and AMX working solutions were prepared with ultra-pure water obtained from a Millipore Milli-Q system with resistivity > 18 MΩ cm at room temperature. Potassium hydrogen phthalate (99.5%) used for total organic carbon analyser (TOC) calibration was purchased from Shimadzu, France.

2.2. Electrolytic system

The electrolyses of AMX solutions were performed with a Hameg HM8040 triple power supply at constant current, in a non-divided cylindrical glass cell of 250 mL capacity with magnetic stirring at thermostatically controlled temperature (20 ± 1 °C). The cell was equipped with a stainless steel cathode of 24 cm^2 and a given anode of the same dimensions, placed in a distance of 3.0 cm one from other. Except PbO_2, all anodes materials tested were purchased ready for use (carbon-felt from Carbon-Lorrain (France), carbon-fiber from SGL Group (Germany), carbon-graphite from CECRI (Central

Electrochemical Research Institute, Karaikudi, Tamilnadu – India), Pt from Platecxis (France), mixed metal oxide Ti/RuO_2-IrO_2 (DSA (Dimensionally Stable Anode) from Baoji Xinyu GuangJiDian Limited Liability Company (China), and BDD (Boron-Doped Diamond) from from Condias GmbH, (Germany)). The PbO_2 was prepared from 2 mm thick lead plates of purity 99.5%. Lead plates were thoroughly cleaned and then they were oxidized under 41.6 mA cm^{-2} current density in 0.1 M H_2SO_4 solution for 1.5 h and finally washed with ultra-pure water.

Oxidation of the model compound AMX in aqueous solution was carried out at constant temperature (20 ± 1 °C) and at natural solution pH of 5.3 without any pH adjustment under galvanostatic conditions, at various current intensities from 50 to 500 mA (2.08 to 20.83 mA cm^{-2}) for electro-oxidation experiments. Mineralization experiments of AMX solutions were conducted at constant current values of 300, 500 and 1000 mA (12.50 to 41.66 mA cm^{-2}). The large current range used for mineralization allowed to study in more details the performance of the process. Aqueous solutions containing 0.1 mM (36.54 mg L^{-1}) AMX and 50 mM Na_2SO_4 were used for electrolysis. Samples were withdrawn during electrolysis at pre-set time intervals to assess the concentration decay of AMX, as well as the mineralization degree of treated solutions.

Cyclic voltammograms were recorded at a constant temperature of 22 ± 1 °C on the different electrodes (glassy carbon, d = 3 mm; Pt, d = 1 mm; for the other large surface electrodes (PbO_2, stainless steel, BDD, DSA) only a height of 1 mm from the lower electrode edge (i.e. an area of ~ 0.4 cm^2) was immersed into the 0.1 M Na_2SO_4 aqueous solution. A Pt foil was used as a counter electrode and the reference electrode was Ag/AgCl. Electrochemical experiments were performed with an EG&G 263A potentiostat/galvanostat and an Echem 4.30 version software.

2.3 Analytical procedures

Concentration decay of AMX was followed by reversed phase HPLC using a Merck Lachrom liquid chromatograph equipped with a quaternary pump L-7100, fitted with a Purospher RP 18, 5 µm, 25 cm x 4.6 mm (id) column at 40° C, and coupled with a L-7455 photodiode array detector selected at optimum wave length of 233 nm. The analysis of AMX decay was carried out isocratically with a mobile phase composed of 0.1% water – methanol 90:10 (v/v) mixture, each solution containing of 1% acetic acid. A flow rate of

0.5 mL min^{-1} was always used. AMX exhibited a well-defined peak at retention time of 14.7 min under these conditions. Samples of 20 µl were injected into the HPLC and measurements were controlled through EZ-Chrom Elite 3.1 software.

The mineralisation extent of electrolysed solutions during AO treatments was assessed from the abatement of their TOC, determined on a Shimadzu TOC-V_{CSH} analyser according to the thermal catalytic oxidation principle.

3. Results and discussion

3.1 Cyclic Voltammetry study of Amoxicillin in aqueous solution

Before studying the anodic oxidation behavior of AMX using different anode materials, we have investigated the cyclic voltammetry behavior of the different anode materials under study in 0.1 M Na_2SO_4 at scan rate of 100 mV s^{-1}. As can be seen in Fig. SM-1, the anodic electroactivity domain is very different following the anode material. This domain is quite well defined for (a) glassy carbon at ~1.7 V vs. Ag/AgCl, (b) platinum at ~1.7 V vs. Ag/AgCl), (d) carbon graphite at ~1.4 V vs. Ag/AgCl, (g) stainless steel at ~1.1 V vs. Ag/AgCl and (h) carbon felt at ~1.4 V vs. Ag/AgCl. But for the other electrodes where a steady increase of the current is observed the definition of the electroactivity domain was difficult.

After recording the electroactivity domain on the different electrodes used in this study, we have investigated the cyclic voltammetry (CV) of AMX on all of these electrodes (Figure SM-2). The only condition under which a signal can be observed is by using a glassy carbon disk, carbon-graphite and carbon felt electrodes with a high concentration of 4 mM of AMX. The irreversible voltammogram at E_{pa} ~ 0.6 V vs. Ag/AgCl is presented on glassy carbon in the Fig. SM-2a.

This voltammogram is in agreement with the literature data: contrary to the penicillin which gives a well-defined CV peak at 1.6 V vs. Ag/AgCl on glassy carbon electrode [46], AMX did not present any CV signal on most unmodified electrodes [47, 48]. However some reports indicated that it is possible to perform an electrochemical determination of AMX under special conditions, i.e. by modification of electrode surface or by derivatization of AMX. For example, Behzad and Damiri [47] obtained an irreversible CV peak for oxidation of AMX at E_{pa} = 0.6 V vs. Ag/AgCl by background-

substracted adsorption stripping voltammetry on glassy carbon electrode modified with multiwalled carbon nanotubes. Conversely, by starting from the quinonic oxidized form of AMX, (obtained by MnO_2 oxidation), Chiu et al. [48] observed a electrochemically reversible system (E_{pa} = 0.6 and a reduction peak at E_{pc} = +0.1 V vs. Ag/AgCl) on a screen-printed carbon electrode in 0.1 M H_3PO_4 solution.

3.2 Comparison of BDD and DSA (Ti/RuO_2-IrO_2) electrodes

The electrochemical data with different anode materials were obtained in an aqueous solution of 0.1 mM (36.54 mg L^{-1}) AMX and 50 mM Na_2SO_4 as supporting electrolyte. Figure 2 shows the decay of the concentration of AMX with time (Fig. 2a) and with the applied current charge (Fig. 2b) during the electrolysis of an AMX solution with DSA and BDD anodes at different current densities ranging from 2.08 to 20.83 mA cm^{-2}. As it can be seen in Fig. 2a, there was a strong influence of the anode material on the oxidation rate of AMX; BDD anode being much faster than the DSA. In fact, the total depletion of AMX was attained with the BDD electrode at 20, 40, and 90 min with an applied current density of 20.83, 12.50 and 4.60 mA cm^{-2}, respectively, whereas with DSA the AMX concentration decay was less than 40% of the initial concentration at 60 min for the higher current value of 20.83 mA cm^{-2} under same operating conditions. As expected, the higher the current density, the higher the oxidation rate of AMX for both electrodes.

Figure 2b shows that the efficiency of the electrolytic processes was also higher for BDD electrode and that it was close to 100% efficiency (according to stoichiometry showing in Eq. (4)) during the initial stage of the process.

$$C_{16}H_{19}N_3O_5S + 40H_2O \rightarrow 16\,CO_2 + 3NO_3^- + SO_4^{2-} + 99\,H^+ + 94\,e^- \qquad (4)$$

Influence of the current density on the efficiency was almost negligible for electrolyses with BDD and DSA; experimental points lay over same trend line in the plot for both anodes, regardless of the current density employed. This was not the expected trend in a direct electrochemical process under mass transfer control (like the one studied because of the very low concentration of pollutant) in which the higher current densities should be clearly less efficient than the lower current densities [49]. This suggests that mediated oxidation must be playing an important role in the overall oxidation process.

Changes in the concentration of AMX are important, but it is worth to take into account that depletion of AMX does not mean total removal of the pollution problem but just an oxidation of the starting species (addition of –OH group) meaning a change in one or some of the functional groups of the molecule, and the formation of intermediates. For this reason, TOC is a much more significant parameter, because it clearly indicates the mineralization of the pollutants, that is, the complete destruction of the starting molecule and its transformation to carbon dioxide.

Figure 3 shows the mineralization of the AMX aqueous solutions. As it can be seen, the reaction times (and, consequently, the current charges applied) required were much higher in these experiments than in the electrolyses shown in Fig. 2. Thus, in the case of AMX, a large number of electrons are needed for the complete mineralization of the molecule up to carbon dioxide, while a simple OH addition may be responsible for the disappearance of AMX and this explains the large electrolysis times in the case of the mineralization study.

Figure 3a clearly indicates that BDD anode was faster than DSA in the mineralization of the AMX, and for both anodes, the higher the current density, the faster the mineralization. However, the effect of the current density for both anodes was much less significant than for simple oxidation of AMX (shown in Fig. 2), suggesting that much more complex processes are occurring during the mineralization process. The reaction times required for complete mineralization of AMX were above 6 h for BDD anode. However, less than 25% of mineralization was obtained for the electrolyses with DSA under the highest current density for this reaction time. Figure 2b indicates again that current density did not influence the efficiency of the mineralization with DSA suggesting a significant role of mediated processes. However, in this case the trends observed for BDD clearly indicated that the process was more efficient working under lower current densities, showing typical behavior of a diffusion controlled process in which a higher current density leads to lower efficiencies due to the occurrence of wasting reactions. Anyway, differences between curves were not very significant (at least they were less significant than expected for a pure mass transfer controlled process) and this indicated that mediated oxidation may be also playing a significant role in this case.

BDD and DSA are usually employed as model anodes to describe the electrolyses of many organic pollutants because they are used to show two opposite behaviors. Thus,

BDD behaves as a high-efficiency electrode for the oxidation of organics. It promotes the mineralization of the organics with an efficiency only limited by mass transport control, and usually few intermediates are observed during the treatment. In addition, it promotes the production of hydroxyl radicals due to its high O_2 evolution overvoltage. On the contrary, DSA electrodes are known as low-efficiency electrodes for the oxidation of organics. These anodes promote a mild oxidation of organics, with a large amount of intermediates (most aromatics treated by these anodes are slowly degraded due to the generation of hardly oxidizable carboxylic acids), a small mineralization and in some cases with production of polymers (particularly, under high concentration of pollutants) [17]. They produce a very low current efficiency and consequently small perspectives of application. An additional difference between DSA and BDD is related to the production of oxidants. With BDD anodes, hydroxyl radicals are available to be combined with sulfate, forming sulfate radical and mono and diperoxosulfate which may extend the oxidation from the nearness of the electrode surface to the bulk. Contrariwise, with DSA these radicals are produced but they are consumed in other processes (reversible oxidation of the electrode components) before they can oxidize sulfate anions to sulfate radicals. This means that finally they are transformed into oxygen and this helps to explain the lower efficiency observed. Platinum and carbon based electrodes as anodes in electro-oxidation can be included into this second type of electrodes because they usually exhibit low-efficiency for the oxidation of organics compared to BDD electrode. Low efficiencies were even more significant with the use of carbon-based materials as anode because they can also be electrochemically incinerated (transformed into carbon dioxide) during the electrochemical process when using high voltages to oxidize organic pollutants. On the other side, the lead dioxide behaved as BDD and performed high efficiency oxidations.

3.3 Comparison of the oxidation capacity of different anode materials

In order to compare the performance of different electrodes studied in this work namely BDD, DSA, PbO_2, Pt, carbon-felt, carbon-graphite and carbon-fiber for the particular case of the oxidation of AMX, the time course during electrolyses were fitted to a pseudo-first order kinetic model by fitting TOC vs. time data to an exponential equation resulting from the integration of the mass balances of the discontinuous cell (Eq.

(5)) in which $[C]_{bulk}$ stands for the concentration of pollutant in the bulk solution in terms of TOC (mineralization).

$$\frac{d[C]_{bulk}}{dt} = k_{app} \cdot [C]_{bulk} \quad (5)$$

This type of model is widely proposed with great success in the literature to model in a simple way the pure direct and mediated electrochemical processes. Fundamentals of this application are going to be further described afterwards relating the apparent (or observed) rate constant, k_{app}, with direct and mediated oxidation pathways.

Using this model, Fig. 4 shows the k_{app} for electro-oxidation of AMX obtained by mathematical fitting of experimental results, respectively [5, 10, 20, 28]. Regression coefficients (R^2) were always above 0.97 indicating the good fitting of experimental results to the first order approach.

It should be remarked that the linear approach was only for the initial stage of the oxidation (for the 20 first min of electrolysis), when the oxidation of intermediates did not significantly compete with that of AMX, because it is the organic molecule with the highest concentration and hence it suffers the largest changes in the concentration. Thus, in the semi-logarithmic plot two zones can be clearly observed (not shown in figure); the first one in which only AMX is oxidized and the second one in which significant concentration of intermediates are present in the system and that should not be used in the calculation of the slope.

Regarding the oxidation rate constants, it can be clearly observed that the process rate increases with the current density for each case (except for the carbon-felt in which a strange shape can be observed), but the slopes were very different depending on the nature of the anode material tested. Low concentrations of AMX employed make us suspect that the process was under mass transport control. To confirm this, a simple ferro-ferricyanide mass transfer determination test was carried out following a procedure described in the literature [50, 51]. Mass transfer coefficient (K_L) for BDD electrode was found as 6.12 x 10^{-5} m s^{-1}. Taking into account this value, it was obtained that the limit current density (j_{lim}) for the initial concentration of AMX (0.1 mM or 36.5 mg/dm^3) and the lowest electron transfer that AMX could suffer (2 electron) would be 0.0295 mA cm^{-2} ($j_{lim}= n \cdot F \cdot K_L \cdot C$) clearly below the range of current densities assessed in this work (2.08

to 20.83 mA cm^{-2}). This confirms that, under our conditions, the current is above the diffusion limit and that the process is therefore controlled by the diffusion kinetics.

In the case of the carbon-felt, due to its large porosity, the electrode surface is much larger than that of other electrodes and this may help to explain the better performance of this electrode in the range of oxidation current densities ranging from 1 to 10 mA cm^{-2}, although it does not explain the increase of the rate with the current density. At this point, it is interesting to take in mind that an estimation of the active area (A) can be obtained by comparison of the K_L x A values obtained in the ferro-ferricyanide test for carbon-felt and BDD electrodes. This comparison resulted in an active surface area for carbon-felt 4.1 times larger than for other electrodes.

Diffusion controlled processes in electrochemical wastewater treatment use to be modeled with first order kinetics assuming they behave as direct oxidation electrochemical processes in which the concentration of pollutant on the surface of the anode is 0. In study this study, CV experiments demonstrated that it is not the case, because the electrochemical oxidation of AMX leads, at the best, to its transformation into an ethylidene quinone Q and because on most electrodes no current is observed in the electroactivity domain of water. However, mediated processes occurring in the vicinity of the electrode surface with very powerful oxidants reagents should provide first order kinetics, because the lifetime of this reagent (•OH) is very short and does not permit its transport far away from the electrode surface. This is the case of •OH mediated oxidations, which clearly behave as direct processes from the mass transfer point of view. Taking into account this fact, the maximum rate of direct oxidation should be given by the mass transport rate (Eq. (6)) [52].

$$r_{direct\ electrochemical\ process} = \frac{I_{limit}}{n \cdot F} = K_L \cdot A \cdot [C]_{bulk} \qquad (6)$$

According to this kinetic model, neither the anode material nor the current density should influence on the electrolyses, because K_L is not affected by any of these parameters. However, this is not the case for k_{app}, (see Fig. 4) in which larger current densities improved the results of the oxidation, and anode material showed a great influence on the results. This means that in addition to this direct-like electrochemical process, a mediated oxidation by electro-generated oxidants should take place. Initially, the rate of this process should be modeled by a second order kinetic (Eq. (7)), although

in electrolytic wastewater treatment processes, the concentration of oxidants ([Ox]) can be assumed to meet a pseudo-steady state value (Eq. (8)), and this allows to simplify the kinetics to a simple first-order equation (Eq. (9)) [52, 53].

$$r_{mediated\ electrochemical\ process} = k_{ox} \cdot [Ox] \cdot [C]_{bulk} \quad (7)$$

$$r_{mediated\ electrochemical\ process} = \left(k_{ox}[Ox]_{pseudo-ss)}\right) \cdot [C]_{bulk} \quad (8)$$

$$r_{mediated\ electrochemical\ process} = k_{mediated} \cdot [C]_{bulk} \quad (9)$$

This new kinetic contributes to the overall oxidation process rate and can help to explain the experimental results. Thus, under mass transfer control, two different kinetic equations should be considered and added in order to define the anodic oxidation and explain the observed values for k_{app}. Taking into account both the equations associated to direct and to mediated processes, a mass balance (Eq. (10) to the discontinuous reactor in which the wastewater treatment is done gives a linear model in semi-logarithmic plot (consistent with the experimental observations) as shown in Eq. (11).

$$V\frac{d[C]_{bulk}}{dt} = K_L \cdot A \cdot [C]_{bulk} + k_{mediated} \cdot [C]_{bulk} \cdot V \quad (10)$$

$$Ln\left(\frac{[C]_{bulk}}{[C]_{bulk_0}}\right) = \frac{K_L \cdot A + k_{mediated} \cdot V}{V} t \quad (11)$$

Relating Eq. (5) with Eq. (10), relationship between the fitting parameter k_{app} and $k_{mediated}$ and k_{ox} is obtained (Eq. (12)):

$$k_{app} = \frac{K_L \cdot A + k_{mediated} \cdot V}{V} \quad (12)$$

Equation (12) can be applied to the oxidation of a single compound in a single stage. If applied to a more complex system, it is worth to take in mind that it behaves simply as an approach. It can be used with TOC removal or with the raw pollutant but taking this limitation into account. In this case, $k_{mediated}$ will account for the specific kinetic of the pollutant species considered (different for TOC or pollutant). As k_L x A is determined by the ferro-ferricyanide test, this equation can be used to account for the influence of oxidants, obtaining the value of $k_{mediated}$ from the experimental data fitting. It has to be taken into account that $k_{mediated}$ depends on the oxidation process (k_{ox}) and on the pseudo-steady state concentration of oxidants as already mentioned in Eq. (9).

As oxidant species like $S_2O_8^{2-}$ and H_2O_2 are electrogenerated on electrodes their contribution in the overall value of the rate constant cannot be neglected. Hence, it's the modification of curves with current density can be explained also by an increase in the concentration of oxidants at the pseudo-steady state or by the action of more powerful oxidants with higher kinetic constants. This means that differences between the oxidation rates of AMX shown in Fig. 4 (k_{app}) should be explained not only in terms of the direct electro-oxidation but also by the action of mediated electro-reagents formed on the surface of the electrode. According to this, the production of these electro-reagents promoted at large current densities with most materials except for carbon-graphite and carbon-fiber (in which not a clear increase is observed). Likewise, it was observed that production of oxidants that can oxidize AMX was promoted with carbon-felt, BDD and Pt anodes, but this production was almost negligible for DSA.. Carbon-graphite and carbon-fiber were situated between both behaviors, maybe because of the production of a weak oxidant. At this point, it is worth to take in mind that a strong oxidant can oxidize easily sp^2-carbon of the anode and hence be ineffective in the oxidation of AMX. Regarding the intercept of the graphs (extrapolated value of k_{app} for j = 0 in Fig. 4), it is interesting to see that most of the curves have a tendency to approximately 1.0 min^{-1} except for DSA. This value is much smaller than that calculated according to Eq. (12) (3.52 min^{-1}) and clearly supports that this term is not standing for direct oxidation but for mediated oxidation in the close vicinity of the anode surface. This is in agreement with the results shown by voltammetry and indicates clearly that electrochemical oxidation of large molecules should not only be related to direct electrochemical process but most importantly to mediated processes, both in the vicinity of the electrode surface and in the bulk and that differences observed for different electrodes are caused primarily by the amount and nature of the oxidants produced on the electrode surfaces.

Compared with other works in literature [5, 20, 21], the huge reaction rates observed for carbon-felt are surprising, especially if it is taken into account that it consists of sp^2-carbon. As will be discussed later, these values are not in agreement with the low mineralization rates observed for this material and can only be explained in terms of a double effect: the enhanced direct-like processes because of higher surface area of carbon-felt (as compared with the other electrodes assessed) and also the production of a mild oxidant (most probably hydrogen peroxide), active for oxidation of the molecule but not for depletion till carbon dioxide of sp^2-carbon of the electrode. The decrease in the

kinetic constant observed for larger current densities is due to the destruction of the electrode (it will be discussed later).

3.4 Comparison based on the current efficiency

From the mass balance shown in Eq. (10) it is easy to get Eq. (13) for galvanostatic electrolyses, simply using the ratio between current intensity applied and time:

$$\frac{d[C]_{bulk}}{dq} = \frac{(K_L \cdot A + k_{mediated} \cdot V)}{I} \cdot [C]_{bulk} \quad (13)$$

Taking into account that the first term is the instantaneous current efficiency for galvanostatic electrolyses [54] expressed in terms of mmol of removed pollutant/Ah (Eq. (14)), this equation shows that the changes in the ICE depends linearly (on a semi-logarithmic plot) on the concentration of pollutant to be oxidized and that the slope (specific efficiency) is related to the mass transfer and to the mediated oxidation kinetics. The specific efficiency is a very interesting parameter because it gives information about the efficiency of the process in terms of amount of electrical charge required to oxidize a certain amount of a given molecule and can be used to calculate average efficiencies of electrochemical processes.

$$\text{ICE (mmol pollutant /Ah)} = \frac{d[C]_{bulk}}{dq} \quad (14)$$

Figure 5 shows the changes in the specific efficiency of the oxidation of AMX. As it can be observed, the higher is the current density; the lower is the specific efficiency. Carbon-felt showed the greater efficiencies for low current densities although the negative effect of the current density was more significant than the current density observed for other electrodes. This decrease supports that hydrogen peroxide may be the oxidant involved in the mediated oxidation processes as its occurrence was only promoted within a limited range of current densities (or cell potentials) and high current densities can lead to the formation of less effective oxygen from electrochemical oxidation of hydrogen peroxide. In addition, the much higher active area of this electrode was also responsible of the higher efficiency as it can be clearly seen in Eq. (13). BDD and PbO_2 were more efficient than platinum and carbon (graphite)-based electrodes with the same electrode area. The decrease in the efficiency observed with the current density was lower for BDD anode.

This means that BDD becomes the best material for large current densities because it preserves its ability to generate hydroxyl radicals even at high current densities compared lead dioxide and others. Regarding the low efficiency anodes, platinum showed a good oxidation behavior much better than that observed for carbon-fiber and carbon-graphite. DSA was found to be the less efficient electrode.

Changes of the oxidation reaction rate constants and specific efficiency are important for the initial oxidation of the AMX but they should be even more important for the complete mineralization process. In this case, very different results were obtained with respect to the oxidation of AMX as it is shown in Figs. 6 and 7. Apparent rate constants and current efficiencies in sp^2-carbon based materials (including carbon-felt) fall to an almost zero values and only diamond, platinum and lead dioxide exhibited appreciable values of both parameters. Results shown by PbO_2 were closer to those of platinum than those of diamond which was clearly the best material to mineralize AMX.

Comparing the kinetic rate constants or the efficiency of oxidation and mineralization of AMX, it can be observed that the oxidation of AMX is one order of magnitude above mineralization. This is important because it clearly exhibits that both are different parameters with a very different meaning, mineralization being the main goal in the efficient removal of pollutants from wastewaters, and much more difficult to attain that depletion of the AMX by transformation into its oxidation intermediates. The high efficiencies obtained for BDD should be explained in terms of the production of hydroxyl radicals and large amount of oxidant as it has been widely described in the literature. Hence, in addition to hydrogen peroxide and ozone, persulfates are expected to play an important role in the oxidation of organic pollutants [55, 56]. Production of persulfates is also possible with Pt and PbO_2 anodes but in a lesser extent [49]. Effect of hydroxyl radicals in direct electrolyses is included in the mass transport kinetic, but its important role in the production of oxidants may be the responsible for the large production of oxidants with BDD anode.

Figure 8 shows an assessment of the mineralization obtained at low current densities with sp^2-carbon based electrodes indicating that only carbon-graphite was robust enough against incineration in the range of low current densities. This is important because carbon-fiber and carbon-graphite were not able to mineralize AMX while they oxidized AMX to intermediates. This means that oxidation intermediates are recalcitrant

to the mineralization with these anode materials. In the case of carbon-felt, the difference was remarkable. It performed very well in the initial oxidation of AMX but it was not able to attain a higher oxidation degree. This confirms the significance of the active area of the electrode and the potential formation of mild oxidants (such as hydrogen peroxide) which help in the initial stages but are not able to mineralize this complex pollutant. Previous results obtained with BDD electrodes with different ratios sp^3/sp^2 during the degradation of enrofloxacin showed that sp^2 carbon in diamond promoted the formation of intermediates [57].

4. Conclusions

A systematic study on the efficiency of the electrode materials such as carbon-felt, carbon-fiber, carbon-graphite, Pt, DSA (Ti/RuO_2-IrO_2), PbO_2, and BDD was carried out through different electrochemical parameters in the oxidative degradation of the drug AMX. First it was evidenced that BDD electrode was more efficient than DSA to oxidize AMX, because the total depletion of the antibiotic was achieved in less than 100 min while less than half of the initial AMX was oxidized with DSA for the best conditions in the same period. The efficiency of the electrolysis versus the current density was closer to 100% for BDD anode during the initial stage of oxidation process indicating that mediated oxidation plays an important role in the whole degradation of AMX. Then, the apparent rate constants of the oxidation reaction of AMX were determined as a function of current densities for several anodes taking into account that the electrochemical process was under mass control. The results showed that apart from BDD electrode, carbon-felt exhibited a better performance for low and moderate current density. Taking into account its porosity and the possibility to generate oxidant species like H_2O_2 leading to the mediated oxidation, we proposed a mathematical model including these phenomena in order to explain its efficiency (in particular at low current densities) compared to other carbon-based materials. On the other hand, the obtained results pointed out that the BDD anode was the best anode material for the large current densities due to generation of high amount of different oxidants: hydrogen peroxide, ozone and persulfates that permits not only the oxidation of AMX but also its complete mineralization.

Acknowledgement

We thank Prof. Hui Zhang (Wuhan University, China) and Dr. S. Vasudevan (Central Electrochemical Research Institute, Karaikudi, Tamilnadu – India) for provide us DSA (Ti/RuO_2-IrO_2) and graphite electrodes respectively. The authors thank Prof. Nesrin Tokay (Hacettepe University) for the English revision. Manuel A. Rodrigo also acknowledges for the invited professor position at Université Paris-Est.

References

[1] A. Bes-Pia, J.A. Mendoza-Roca, L. Roig-Alcover, A. Iborra-Clar, M.I. Iborra Clar, M.I. Alcaina-Miranda, Comparison between nanofiltration and ozonation of biologically treated textile wastewater for its reuse in the industry, Desalination 157 (2003) 81-86.

[2] J. Kim, I. Song, S. Lee, P. Kim, H. Oh, J. Park, Y. Choung, Decompostion of pharmaceuticals (sulfamethazine and sulfathiazole) using oxygen-based membrane biofilm reactor, Desalination 250 (2010) 751-756.

[3] N. K. Pazarlioglu, R. Oztürk Urek, F. Ergun, Biodecolourization of Direct Blue 15 by immobilized Phanerochate chrysosporium, Process Biochem. 40 (2005) 1923-1929.

[4] M. Saquib, M. Muneer, TiO_2-mediated photocatalytic degradation of a triphenylmethane dye (gentian violet), in aqueous suspensions, Dyes Pigments 56 (2003) 37-49.

[5] E. Brillas, I. Sirés and M.A. Oturan, Electro-Fenton process and related electrochemical technologies based on Fenton's reaction chemistry, Chem. Rev. 109 (2009) 6570-6631.

[6] M.A. Oturan, J. Peiroten, P. Chartrin and A.J. Acher, Complete destruction of p-nitrophenol in aqueous medium by electro-Fenton method, Environ. Sci. Technol. 34 (2000) 3474-3479.

[7] M. Pera-Titus, V. Garcia-Molina, M.A. Banos, J. Gimenez, S. Esplugas, Degradation of chlorophenols by means of advanced oxidation processes: a general review, Appl. Catal. B-Environ. 47 (2004) 219-256.

[8] I. Sirés, E. Brillas, Remediation of water pollution caused by pharmaceutical residues based on electrochemical separation and degradation technologies: A review, Environ. Int. 40 (2012) 212-229.

[9] M.A. Oturan, N. Oturan, M. C. Edelahi, F. I. Podvorica and K. El Kacemi, Oxidative degradation of herbicide diuron in aqueous medium by Fenton's reaction based advanced oxidation processes, Chem. Eng. J. 171 (2011)127-135.

[10] A. Dirany, I. Sirés, N. Oturan, A. Özcan and M.A. Oturan, Electrochemical treatment of sulfachloropyridazine: Kinetics, reaction pathways, and toxicity evolution, Environ. Sci. Technol. 46 (2012) 4074-4082.

[11] N. Belhadj, A. Savall, Electrochemical removal of phenol in alkaline solution. Contribution of the anodic polymerization on different electrode materials, Electrochim. Acta 54 (2009) 4809-4816.

[12] P. Canizares, M. Hernandez-Ortega, M.A. Rodrigo, C.E. Barrera-Diaz, G. Roa-Morales, C. Saez, A comparison between conductive-diamond electrochemical

oxidation and other advanced oxidation processes for the treatment of synthetic melanoidins, J. Hazard. Mater. 164 (2009) 120-125.

[13] P. Canizares, J. Lobato, R. Paz, M.A. Rodrigo, C. Saez, Electrochemical oxidation of phenolic wastes with boron-doped diamond anodes, Water Res. 39 (2005) 2687-2703.

[14] N. Oturan, E. Brillas, M.A. Oturan, Unprecedented total mineralization of atrazine and cyanuric acid by anodic oxidation and electro-Fenton with a boron-doped diamond anode, Environ. Chem. Lett. 10 (2012) 165-170.

[15] M. Panizza, G. Cerisola, Applicability of electrochemical methods to carwash wastewaters for reuse. Part 1: Anodic oxidation with diamond and lead dioxide anodes, J. Electroanal. Chem. 638 (2010) 28-32.

[16] A. Kapalka, B. Lanova, H. Baltruschat, G. Foti, C. Comninellis, Electrochemically induced mineralization of organics by molecular oxygen on boron-doped diamond electrode. Electrochem. Commun. 10 (2008) 1215-1218.

[17] M. Panizza, G. Cerisola, Direct and mediated anodic oxidation of organic pollutants, Chem. Rev. 109 (2009) 6541-6569.

[18] B. Louhichi, M.F. Ahmadi, N. Bensalah, A. Gadiri, M.A. Rodrigo, Electrochemical degradation of an anionic surfactant on boron-doped diamond anodes, J. Hazard. Mater. 158 (2008) 430-437.

[19] A. Kapalka, G. Foti, C. Comninellis, The importance of electrode material in environmental electrochemistry. Formation and reactivity of free hydroxyl radicals on boron doped diamond electrodes, Electrochim. Acta 54 (2009) 2018-2023.

[20] N. Oturan, J. Wu, H. Zhang, V.K. Sharma, M.A. Oturan, Electrocatalytic destruction of the antibiotic tetracycline in aqueous medium by electrochemical advanced oxidation processes: Effect of electrode materials, Appl. Catal. B-Environ. 140-141 (2013) 92-97.

[21] C.A. Martinez-Huitle, S. Ferro, Electrochemical oxidation of organic pollutants for the wastewater treatment: direct and indirect processes, Chem. Soc. Rev. 35 (2006) 1324-1340

[22] M. Panizza, G. Cerisola, Application of diamond electrodes to electrochemical processes Electrochim. Acta 51 (2005) 191-199.

[23] K. Serrano, P.A. Michaud, C. Comninelis, A. Savall, Electrochemical preparation of peroxidisulfuric acid using boron doped diamond thin film electrodes, Electrochim. Acta 48 (2002) 431-436.

[24] P. Canizares, C. Saez, A. Sanchez-Carretero and M.A. Rodrigo, Synthesis of novel oxidants by electrochemical technology, J. Appl. Electrochem. 39 (2009) 2143-2149.

[25] E. Brillas, I. Sirés, C. Arias, P.L. Cabot, F. Centellas, R.M. Rodriguez, J.A. Garrido, Mineralization of paracetamol in aqueous medium by anodic oxidation with a boron-doped diamond electrode, Chemosphere 58 (2005) 399-406.

[26] A. Özcan, Y. Şahin, A.S. Koparal, M.A. Oturan, Propham mineralization in aqueous medium by anodic oxidation using boron-doped diamond anode. Experimental parameters' influence on degradation kinetics and mineralization efficiency, Water Res. 42 (2008) 2889-2898.

[27] V. Santos, J. Diogo, M.J.A. Pacheco, L. Ciriaco, A. Morao, A. Lopes, Electrochemical degradation of sulfonated amines on SI/BDD electrodes, Chemosphere, 79 (2010) 637-645.

[28] S. Loaiza-Ambuludi, M. Panizza, N. Oturan, A. Özcan, M.A. Oturan, Kinetic behavior of anti-inflammatory drug ibuprofen in aqueous medium during its oxidation by electrochemical advanced oxidation, Environ. Sci. Pollut. R. 20 (2013) 2381-2389.

[29] M. Panizza, G. Cerisola, Removal of colour and COD from wastewater containing acid blue 22 by electrochemical oxidation, J. Hazard. Mater. 153 (2008) 83-88.

[30] S. Garcia-Segera, E. Brillas, Mineralisation of the recalcitrant oxalic and oxamic acids by electrochemical advanced oxidation processes using a boron-doped diamond anode, Water Res. 45 (2011) 2975-2984.

[31] S. Hammami, N. Bellakhal, N. Oturan, M.A. Oturan, M. Dachraoui, Degradation of Acid Orange 7 by electrochemically generated •OH radicals in acidic aqueous medium using a boron-doped diamond or platinum anode. A mechanistic study, Chemosphere 73 (2008) 678-684.

[32] [34] B. Marselli, J. Garcia-Gomez, P-A. Michaud, M.A. Rodrigo, C. Comninellis, Eelectrogeneration of hydroxyl radicals on boron-doped diamond electrodes, J. Electrochem. Soc. 150 (2003) 79-83.

[33] M. Panizza, I. Sirés and G. Cerisola, Anodic oxidation of mecoprop herbicide at lead dioxide, J. Appl. Electrochem. 38 (2008) 923-929.

[34] M. Panizza and G. Cerisola, Influene of anode material on the electrochemical oxidation of 2-naphthol: Part 2. Bulk electrolysis experiments, Electrochim. Acta 49 (2004) 3221-3226.

[35] O. Sialdone, A. Galia, G. Filardo, Electrochemical incineration of 1.2-dichloroethane: Effect of the electrode material, Electrochim. Acta 53 (2008) 7220-7225.

[36] C.A. Martinez-Huitle, S. Ferro, A. De Battisti, Electrochemical incineration of oxalic acid: Role of electrode material, Electrochim. Acta 49 (2004) 4027-4034.

[37] S. Ammar, M. Asma, N. Oturan, R. Abdelhedi, M.A. Oturan, Electrochemical degradation of anthraquinone dye Alizarin Red: Role of the electrode material, Curr. Org. Chem. 16 (2012) 1978-1985.

[38] J. Iniesta, P.A. Michaud, M. Panizza, G. Cerisola, A. Aldaz, C. Comninellis, Electrochemical oxidation of phenol at boron-doped diamond electrode, Electrochim. Acta 46 (2001) 3573-3578.

[39] A.M. Palcaro, S. Palmas, F. Renoldi, M. Mascia, On the performance of Ti/SnO_2 and Ti/PbO_2 anodes in electrochemical degradation of 2-chlorophenol for wastewater tretment, J. Appl. Electrochem. 29 (1999) 147-151.

[40] C. Flox, J.A. Garrido, R.M. Rodriguez, F. Centellas, P-L. Cabot, C. Arias, E. Brillas, Degradation of 4.6-dinitro-o-cresol from water by anodic oxidation with a boron-doped diamond electrode, Electrochim Acta 50 (2005) 3685-3692.

[41] J. Rodrigez, M.A. Rodrigo, M. Panizza and G. Cerisola, Electrochemical oxidation of Acid Yellow 1 using diamond anode, J. Appl. Electrochem. 39 (2009) 2285-2289.

[42] E. Chatzisymeon, S. Fierro, I. Karafyllis, D. Mantzavinos, N. Kalogerakis, A. Katsaounis, Anodic oxidation of phenol on Ti/IrO_2 electrode: Experimental studies, Catal. Today 151 (2010) 185-189.

[43] C. Flox, C. Arias, E. Brillas, A. Savall, K. Groenen-Serrano, Electrochemical incineration of cresols: A comparative study between PbO_2 and boron-doped diamond anodes, Chemosphere 74 (2009) 1340-1347.

[44] K. Kummerer, Antibiotics in the aquatic environment - a review - part I, Chemosphere 75 (2009) 417–434.

[45] T. Heberer, Occurrence, fate, and removal of pharmaceutical residues in the aquatic environment: a review of recent research data, Toxicol. Lett. 131 (2002) 5–17.

[46] L. Svorc, J. Sochr J., M. Rievaj, P. Tomcik, D. Bustin, Voltammetric determination of penicillin V in pharmaceutical formulations and human urine using a boron-doped diamond electrode, Bioelectrochemistry 88 (2012) 36-41.

[47] B. Rezaei, S. Damiri, Electrochemistry and adsorptive stripping voltammetric determination of amoxicillin on a multiwalled carbon nanotubes modified glassy carbon electrode, Electroanal. 21 (2009) 1577-1586.

[48] M.H. Chiu, J.L. Chang, J.M. Zen, An analyte derivatization approach for improved electrochemical detection amoxicillin, Electroanal. 21 (2009) 1562-1567.

[49] J.M. Aquino, M.A. Rodrigo, R.C. Rocha-Filho, C. Saez, Cañizares, Influence of the supporting electrolyte on the electrolyses of dyes with conductive-diamond anodes, Chem. Eng. J. 184 (2012) 221-227.

[50] P. Cañizares, J. García-Gómez, I. Fernández de Marcos, M.A. Rodrigo, J. Lobato, Measurement of mass-transfer coefficients by an electrochemical technique, J. Chem. Edu. 83 (2006) 1204-1207.

[51] M.A. Rodrigo, P.A. Michaud, I. Duo, M. Panizza, G. Cerisola, Ch. Comninellis, Oxidation of 4-chlorophenol at Boron-Doped Diamond electrode for wastewater treatment, J. Electrochem. Soc. 148 (2001) D60-64.

[52] P. Cañizares, J. García-Gómez, J. Lobato, M.A. Rodrigo, Modeling of wastewater electro-oxidation processes part I. General description and application to inactive electrodes, Ind. Eng. Chem. Res. 43 (2004) 1915-1922.

[53] P. Cañizares, J. García-Gómez, J. Lobato, M.A. Rodrigo, Modeling of wastewater electro-oxidation processes, part II. Application to active electrodes, Ind. Eng. Chem. Res. 43 (2004) 1923-1931.

[54] F.L. Souza, C. Sáez, P. Cañizares, A.J. Motheo, M.A. Rodrigo, Sonoelectrolysis of wastewaters polluted with dimethyl phthalate, Ind. Eng. Chem. Res. 52 (2013) 9674−9682.

[55] P. Canizares, C. Saez, A. Sanchez-Carretero, M.A. Rodrigo, Synthesis of novel oxidants by electrochemical technology. J. Appl. Electrochem. 39 (2009) 2143-2149.

[56] K. Serrano, P.A. Michaud, C. Comninellis, A. Savall, Electrochemical preparation of peroxodisulfuric acid using boron doped diamond thin film electrodes. Electrochimica Acta 48 (2002) 431-436.

[57] E. Guinea, F. Centellas, E. Brillas, P. Canizares, C. Saez and M.A. Rodrigo, Electrocatalytic properties of diamond in the oxidation of a persistent pollutant, Appl. Catal. B-Environ. 89 (2009) 645-650.

Figures captions

Figure 1. Chemical structure of AMX.

Figure 2. Effect of current density on the oxidation of AMX with DSA (○: 2.08; □: 4.60; △: 12.50; and ◇: 20.83 mA cm^{-2}) and BDD (●: 2.08; ■: 4.60; ▲: 12.50; and ◆: 20.83 mA cm^{-2}) anodes. Dashed line: 100% efficiency according to Faraday law for total oxidation of AMX. (a) changes versus time; (b) changes versus electrical charge. Raw AMX solution: 0.1 mM AMX, 50 mM Na_2SO_4, pH 5.3. Room temperature.

Figure 3. Effect of current density on the mineralization of AMX with DSA (○: 12.50 mA cm^{-2} ; □: 20.83 mA cm^{-2} ; and △: 41.66 mA cm^{-2}) and BDD anodes (●: 12.50 mA cm^{-2} ; ■: 20.83 mA cm^{-2}; and ▲: 41.66 mA cm^{-2}). (a): TOC changes versus time. (b): TOC changes versus electrical charge. Raw AMX solution: 0.1 mM AMX, 50 mM Na_2SO_4, pH 5.3. Room temperature.

Figure 4. Effect of current density on the rate of oxidation of AMX with different anode materials: Pt (∗); PbO_2 (□); DSA (△); carbon-fiber (■); carbon-graphite (◆); carbon-felt (●); and BDD (▲).Raw AMX solution: 0.1 mM AMX, 50 mM Na_2SO_4, pH 5.3. Room temperature. Applied current density within the range 2.08-20.83 mA cm^{-2}

Figure 5. Change in current efficiency during electrolysis of AMX aqueous solutions with different anode materials: Pt (∗); PbO_2 (□); DSA (△); carbon-fiber (■); carbon-graphite (◆); carbon-felt (●); and BDD (▲).Raw AMX solution: 0.1 mM AMX, 50 mM Na_2SO_4, pH 5.3. Room temperature. Applied current density within the range 2.08-20.83 mA cm^{-2}

Figure 6. Effect of current density on the rate of mineralization of AMX with different anode materials: Pt (∗); PbO_2 (□); DSA (△); carbon-fiber (■); carbon-graphite (◆); carbon-felt (●); and BDD (▲). Raw AMX solution: 0.1 mM AMX, 50 mM Na_2SO_4, pH 5.3. Room temperature. Applied current density within the range 12.50-41.66 mA cm^{-2}. Onset: Details of the fitting procedure for the experiments carried out with BDD.

Figure 7. Changes of current efficiency during mineralization of AMX with different anode materials: Pt (∗); PbO_2 (□); DSA (△); carbon-fiber (■); carbon-graphite (◆); carbon-felt (●); and BDD (▲).Raw AMX solution: 0.1 mM AMX, 50 mM Na_2SO_4, pH 5.3. Room temperature. Applied current density within the range 12.50-41.66 mA cm^{-2}.

Figure 8. Characterization of the mineralization at low current densities with sp2-carbon anodes: (■, □): carbon-graphite, (◆, ◊): carbon-fiber, (▲, △): carbon-felt. Empty symbols: First order constant rates for mineralization (k_{app}). Full symbols: ICE. Raw AMX solution: 0.1 mM AMX, 50 mM Na_2SO_4, pH 5.3. Room temperature.

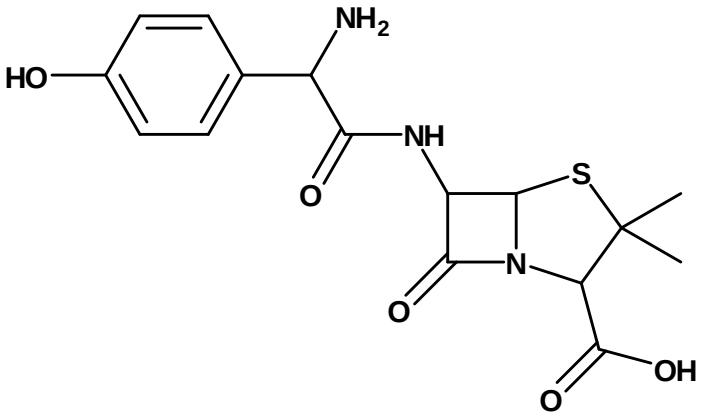

Figure 1

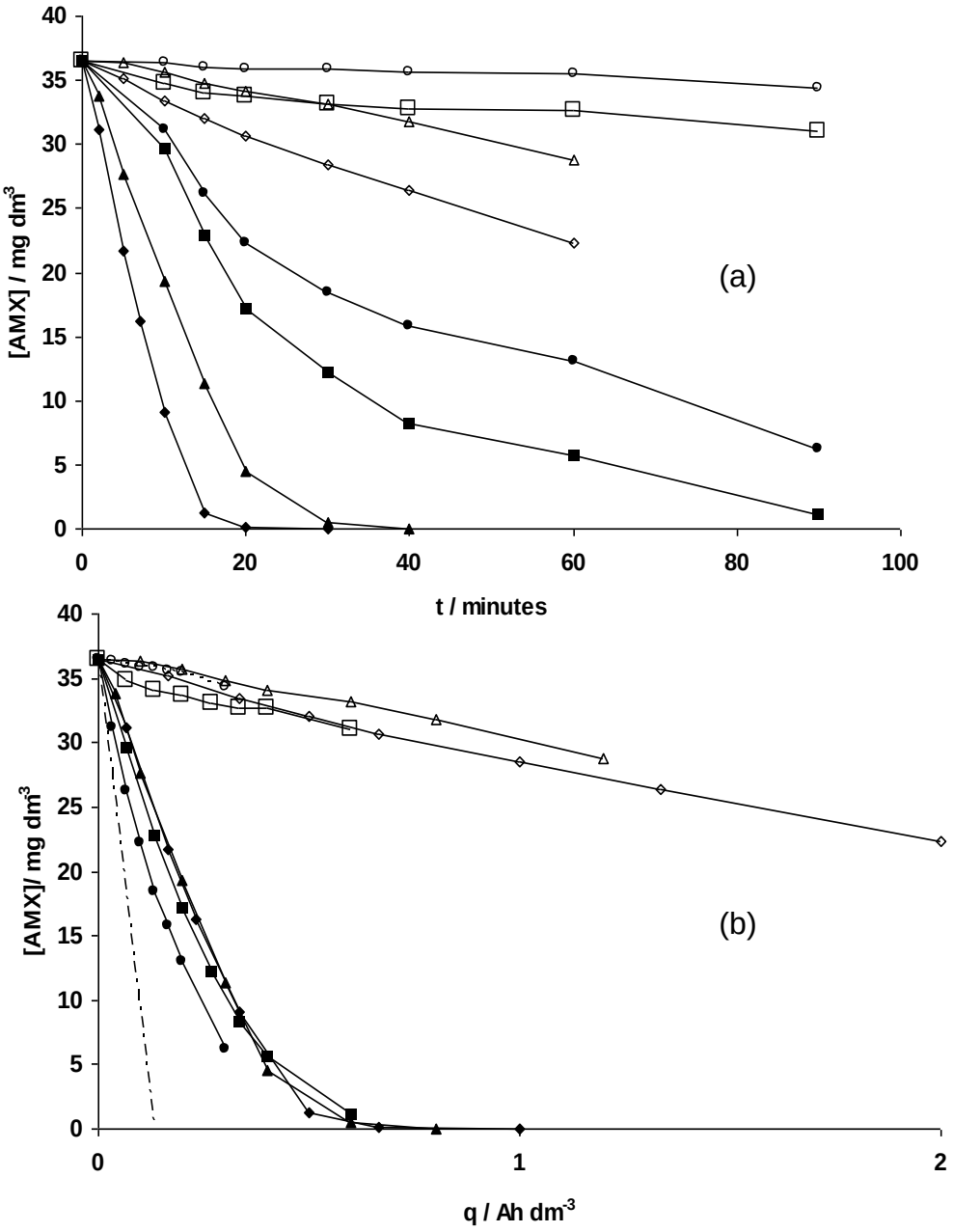
40
35
30
25
20
15
10
5
0
[AMX] / mg dm-3
(a)
0
20
40
60
80
100
t / minutes
40
35
30
25
20
15
10
5
0
[AMX]/ mg dm-3
(b)
0
1
2
q / Ah dm-3

Figure 2

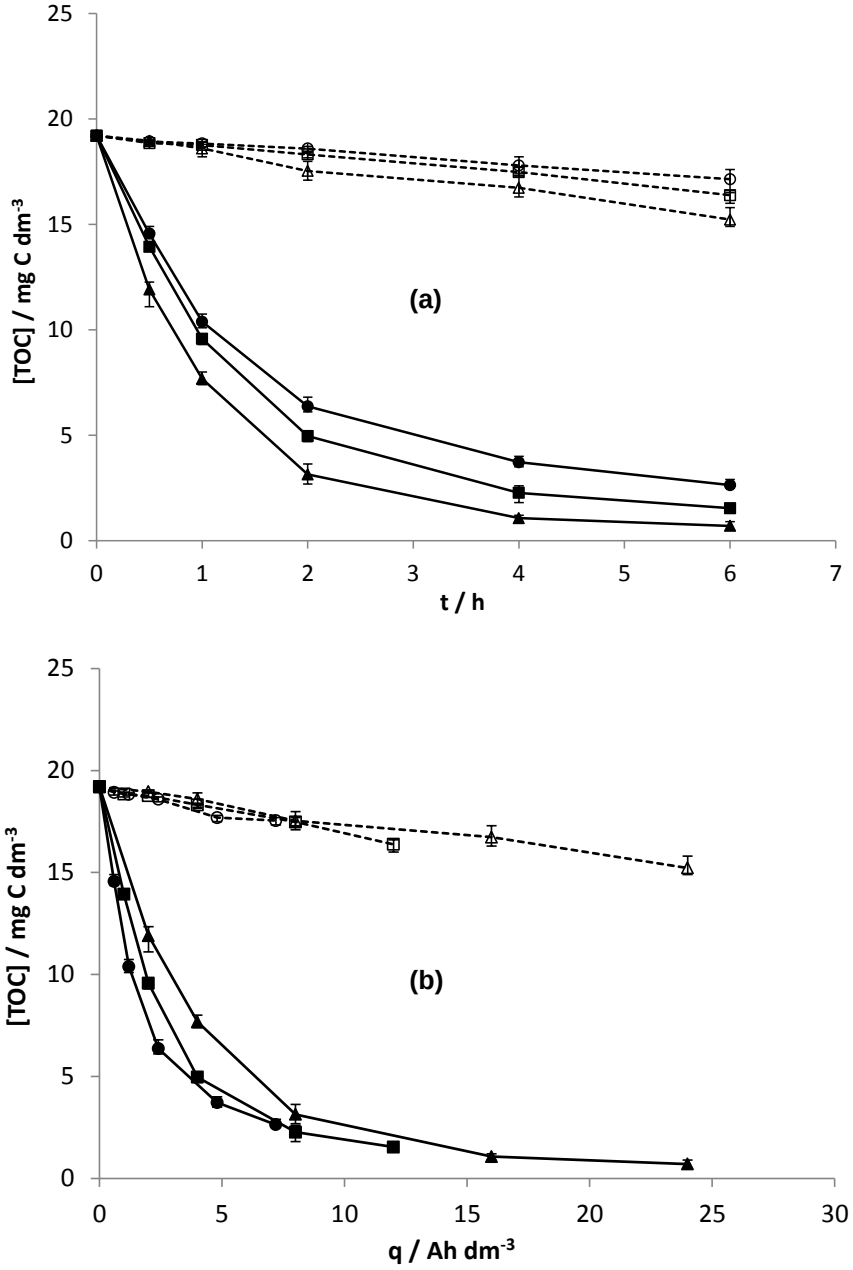
25
20
15
10
5
0
[TOC] / mg C dm-3
(a)
0
1
2
3
4
5
6
7
t / h
25
20
15
10
5
0
[TOC] / mg C dm-3
(b)
0
5
10
15
20
25
30
q / Ah dm-3

Figure 3

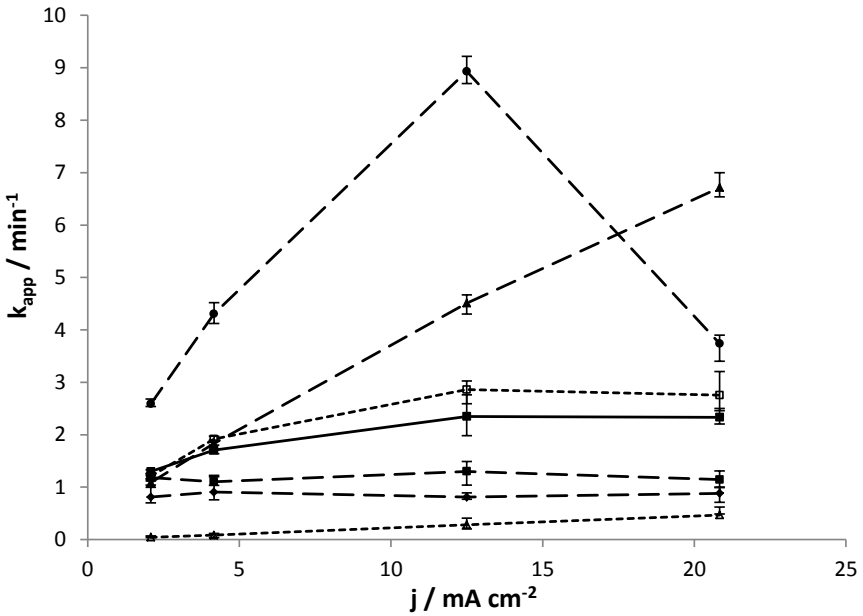

Figure 4

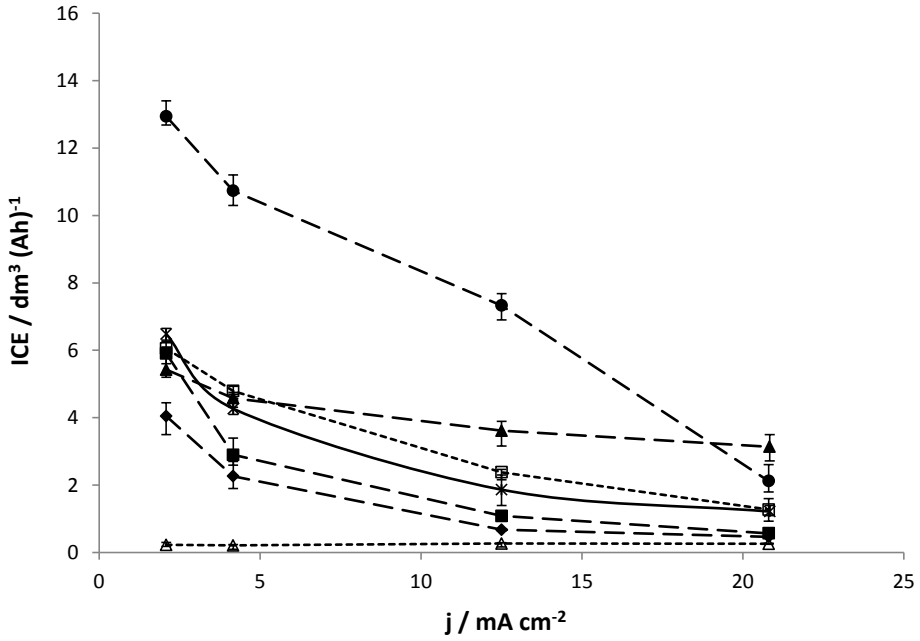

Figure 5

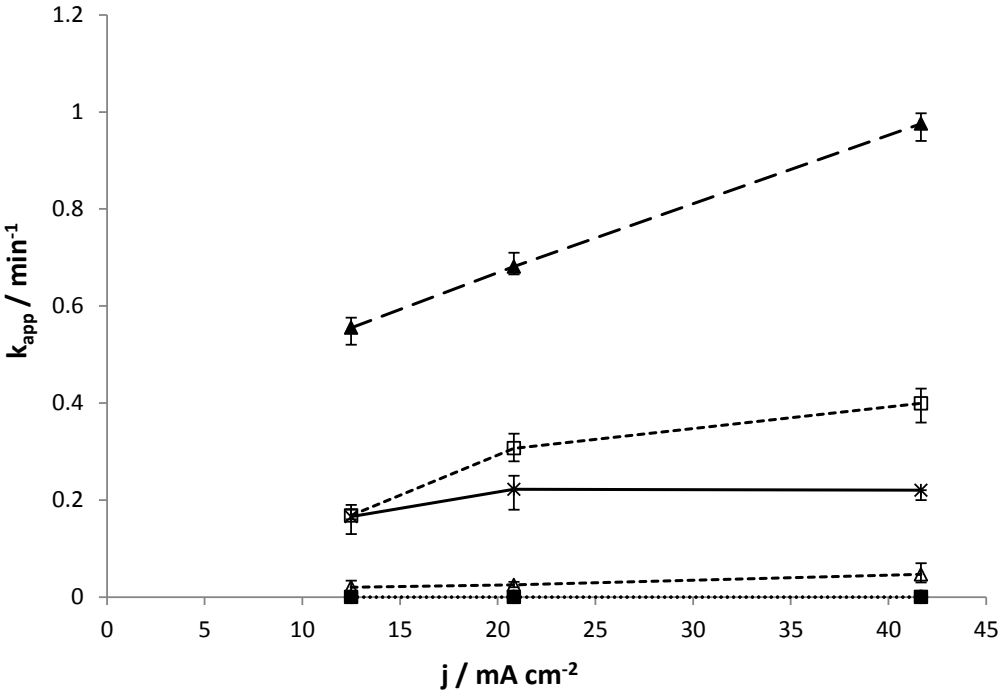

Figure 6

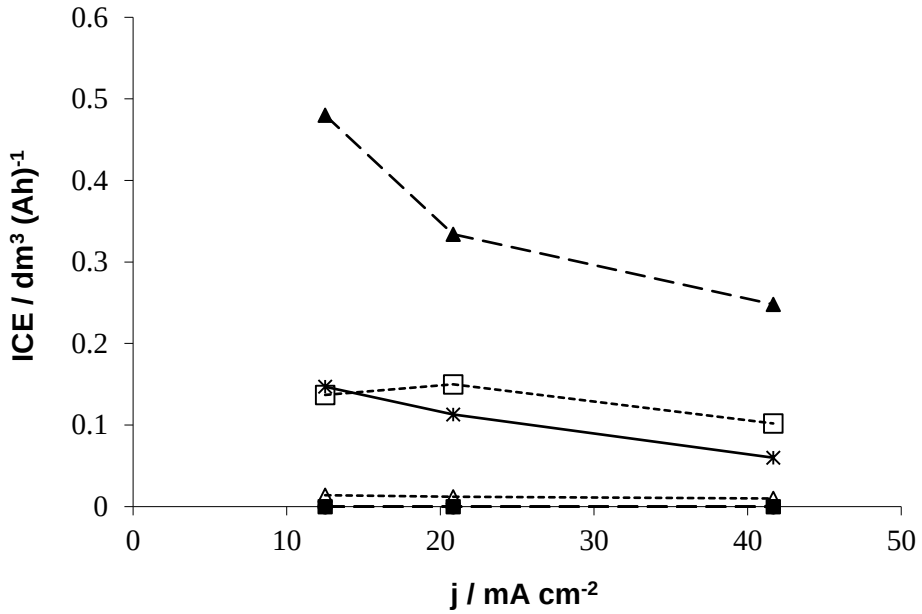

Figure 7

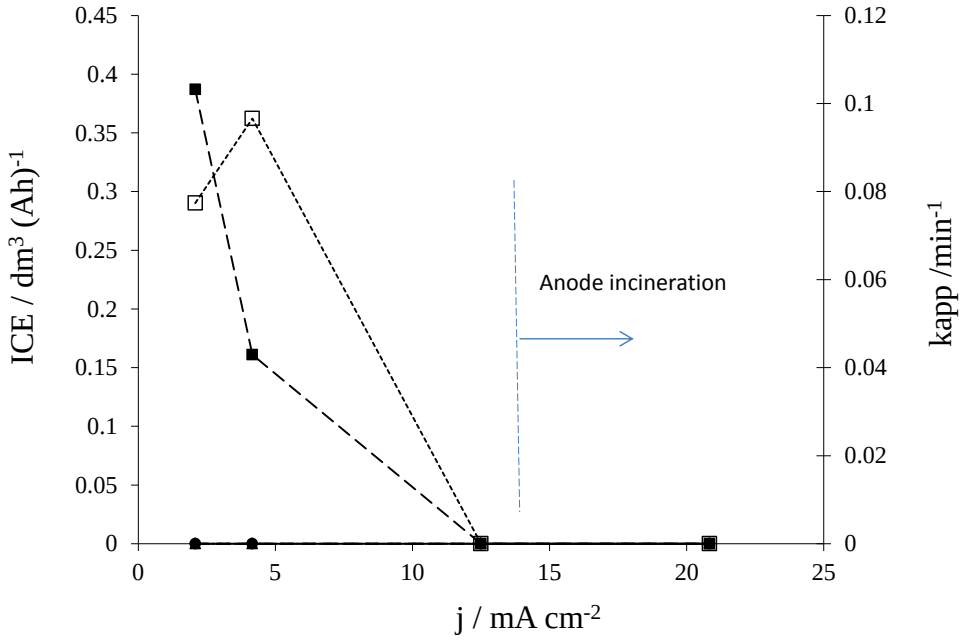
0.45
0.4
0.35
0.3
0.25
0.2
0.15
0.1
0.05
0
ICE / dm3 (Ah)-1
0.12
0.1
0.08
0.06
0.04
0.02
0
kapp /min-1
Anode incineration
0
5
10
15
20
25
j / mA cm-2

Figure 8